Zhang *et al.*
Cell Communication and Signaling (2024) 22:579
https://doi.org/10.1186/s12964-024-01950-x

Cell Communication and Signaling

RESEARCH

Open Access

Atg5-deficient mesenchymal stem cells protect against non-alcoholic fatty liver by accelerating hepatocyte growth factor secretion

Caifeng Zhang[1*], Juanjuan Ji[1,2], Xuefang Du[1,2], Lanfang Zhang[1,2], Yaxuan Song[1,2], Yuyu Wang[1,2], Yanan Jiang[3], Ke Li[1,2] and Tingmin Chang[1,2*]

Abstract

Background/aims Mesenchymal stem cells (MSCs) have shown promising therapeutic potential in treating liver diseases, such as non-alcoholic fatty liver disease (NAFLD). Genetic modification has been employed to enhance the characteristics of MSCs for more effective disease treatment. Here, we present findings on human adipose-derived MSCs with Atg5 deficiency, investigating their therapeutic impact and the associated mechanisms in NAFLD.

Methods In vitro, lentiviral transduction was employed to downregulate Atg5 or HGF in human adipose-derived MSCs using short hairpin RNA (shRNA). Subsequently, experiments were conducted to evaluate cell senescence, proliferation, cell cycle, apoptosis, and other pertinent aspects. In vivo, a non-alcoholic fatty liver mouse model was established by feeding them a high-fat diet (HFD), and the effects of MSCs transplantation were assessed through serological, biochemical, and pathological analyses.

Results Our research findings indicate that Atg5-deficient MSCs display heightened proliferative activity. Subsequent co-culturing of MSCs with hepatocytes and the transplantation of Atg5-deficient MSCs into NAFLD mouse models demonstrated their ability to effectively reduce lipid accumulation in the NAFLD disease model by modulating the AMPKα/mTOR/S6K/Srebp1 pathway. Furthermore, we observed that Atg5 deficiency enhances the secretion of hepatocyte growth factor (HGF) by promoting recycling endosome (RE) production. Lastly, our study revealed that 3-MA-primed MSCs can improve the characteristics of NAFLD by boosting the secretion of HGF.

Conclusions Our research findings suggest that Atg5-deficient MSCs protect against NAFLD by accelerating HGF secretion. This indicates that Atg5 gene-modified MSCs may represent a promising strategy for treating NAFLD.

Keywords Mesenchymal stem cells, Non-alcoholic fatty liver disease, Atg5, Recycling endosomes, HGF

*Correspondence:
Caifeng Zhang
zhangcaifeng666@163.com
Tingmin Chang
ctminmail@163.com
Full list of author information is available at the end of the article

Introduction

Non-alcoholic fatty liver disease (NAFLD) is a liver condition characterized by the abnormal accumulation of fat in the liver due to various factors, including genetic predisposition, obesity, high cholesterol, hypertension, diabetes, or other metabolic disorders [1, 2]. NAFLD can progress to non-alcoholic steatohepatitis (NASH), liver fibrosis, cirrhosis, and potentially even liver cancer. Unfortunately, there are currently no approved pharmaceutical treatments for NASH [2, 3]. Therefore, there is a pressing need for more effective therapies to prevent the progression of liver steatosis to chronic liver disease.

Mesenchymal stem cells (MSCs) have demonstrated promising therapeutic potential in various diseases, including NAFLD [4]. Their beneficial effects include inhibiting fatty acid synthesis, boosting lipid oxidation, enhancing hepatic glycogen synthesis, and regulating immune cell functions [5–7]. However, the limited survival duration of MSCs in the body can impact their effectiveness [8]. Recent research has focused on enhancing the paracrine activity, immunoregulatory capacity, and in vivo persistence of MSCs through genetic modifications and pre-treatments with medications [9]. By targeting key proteins involved in critical cellular processes such as cell survival, apoptosis, inflammation, and regeneration, including genes like IL-1β, Bcl-2, and hepatocyte growth factor (HGF), researchers aim to improve the therapeutic potential of engineered MSCs in treating liver diseases [4]. This advancement signifies a promising approach for effective liver disease treatment.

Autophagy is a crucial cellular process that coordinates the degradation and recycling of cellular components within mammalian cells through the lysosomal system [10]. By removing damaged organelles, misfolded proteins, and other unnecessary or dysfunctional cellular elements, autophagy plays a central role in maintaining cellular homeostasis [11, 12]. Importantly, recent research highlights the crucial role of autophagy in regulating endosome sorting processes. Studies have demonstrated that the formation of the double-membrane structure in autophagosomes originates from various cellular membranes, including the plasma membrane, endosomes, and the endoplasmic reticulum [13]. Disruptions in autophagic activity can significantly affect the efficiency and volume of intracellular sorting processes, highlighting the intricate relationship between autophagy and endosome homeostasis [14, 15]. Studies have demonstrated that the activation of autophagy can result in significant degradation of endosomes targeted for capture by vesicles, impacting the recycling of specific receptors, such as the EGFR [16, 17].

In MSCs, the inhibition of autophagy has been shown to enhance cell proliferation and suppress apoptosis, thereby prolonging their survival in transplanted mice [8]. The role and potential mechanism of autophagy-modulated MSCs in NAFLD remain unclear. In this study, we established a long-term high-fat diet (HFD)-induced NAFLD mouse model and evaluated the effects by transplanting MSCs. In vitro, we co-cultured MSCs with hepatocytes to evaluate their influence on hepatic lipid metabolism. Ultimately, we found that autophagy-deficient MSCs enhanced HGF secretion by accelerating the generation of recycling endosomes (REs), thereby modulating the AMPKα/mTOR/S6K/Srebp1 signaling to ameliorate NAFLD.

Materials and methods

Cell culture and treatment

The primary human adipose-derived MSCs (CP-H202) were obtained from Procell (China) and cultured in a medium containing 10% fetal bovine serum (FBS) (Gibco), 1% penicillin/streptomycin (Gibco), and Dulbecco's Modified Eagle's Medium (DMEM) (Hyclone). Human HepG2 cells and Mouse AML12 cells were purchased from the Type Culture Collection of the Chinese Academy of Sciences, Shanghai, China. The liver cells were cultured in H-DMEM medium supplemented with 10% FBS and 1% penicillin–streptomycin. All cells were maintained in a cell incubator at 37 °C under a 5% CO2 atmosphere with water-saturated conditions. The MSCs in passages 2 or 3 were utilized for co-culture with hepatocytes, whereas cells in passages 4–5 were employed for cell transplantation in HFD-fed mice.

The lipid accumulation model in hepatocytes is established by treating the cells with 400 μM free fatty acids (FFAs), which consist of a 2:1 mixture of oleic acid (O1008, Sigma) and palmitic acid (P5585, Sigma), dissolved in a BSA solution, for 24 h. After this treatment, further experiments are conducted. Additionally, 3-methyladenine (3-MA, S2767, Selleck), an inhibitor of autophagosome formation, is applied at a concentration of 5 mM to treat MSCs, while chloroquine (CQ, S6999, Selleck), which blocks autophagosome–lysosome fusion, is applied at a concentration of 10 mM to treat MSCs prior to further experimentation.

Animals and treatment

Male C57BL/6 mice (8 weeks old) were obtained from Vital River Laboratories in Beijing, China, and were housed under specific pathogen-free conditions with a 12-h light–dark cycle. A mouse model of NAFLD was induced by feeding the mice a HFD consisting of 19.4% protein, 60% fat, and 20.6% carbohydrates (TP23300, Trophic, Jiangsu, China). Mice fed a normal chow diet (NCD) (LAD3001M, Trophic, Jiangsu, China) were used as controls. After 8 weeks on the HFD, the mice received

the first MSCs transplantation (1×10^6 cells/mouse) via the tail vein. A total of 3 injections were administered at 2-week intervals. The mice were sacrificed for analysis 4 weeks after the final injection. The experimental protocols were reviewed and approved by the Ethics Committee of Xinxiang Medical University, ensuring compliance with animal welfare and ethical principles.

Lentivirus infections

The lentivirus packaging was carried out in a 75 cm^2 dish with appropriate controls and treatments. Prior to lentivirus packaging, the medium was refreshed, and 293 T cells were transfected with lentivirus plasmids containing shAtg5, shHGF or shGfp (as a non-targeting control). The lentivirus plasmids were mixed with Lipofectamine 3000 (Thermo, L3000015, USA) before being introduced to the 293 T cells. After a 72-h incubation period, the lentivirus particles were harvested, and MSCs were infected at a 1:1 ratio to generate MSC^{shAtg5}, MSC^{shHGF} or MSC^{shGfp}. Puromycin treatment was then used to select and culture the MSCs for subsequent experimentation. The shRNA plasmids were purchased from Santa Cruz (sc-37111, sc-45924, sc-41445).

Quantitative real-time PCR analysis

The specified cells and tissues were washed, harvested, and processed for total RNA extraction using TRIzol Reagent (DP424, Tiangen, China) following the manufacturer's guidelines. The extracted RNA was then reverse transcribed into cDNA using the PrimerScript RT Reagent Kit (KR116, Tiangen, China). All real-time PCR reactions were performed using the SYBR Green reagent kit (FP201, Tiangen, China) and an ABI 7500 real-time PCR system. mRNA expression levels were quantified using the delta-delta CT method, with GAPDH utilized as the internal control. The primer pairs used in this study are listed in Table S1.

Western blot analysis

The cells or mouse tissues were lysed using RIPA lysis buffer (R0010, Solarbio, China) containing protease inhibitor (P6730, Solarbio, China) and phosphatase inhibitor (P1260, Solarbio, China) to extract total protein samples. Protein concentrations were determined utilizing the BCA Protein Assay Kit (PC0020, Solarbio, China). The samples were then loaded onto 10% SDS–polyacrylamide gels and subsequently transferred to PVDF membranes. These membranes were blocked with 5% non-fat milk in PBS for 1 h and incubated with primary antibodies at 4 °C overnight, followed by incubation with HRP-conjugated secondary antibodies. Antibodies were visualized using enhanced chemiluminescence reagent. Protein expression levels were analyzed using Image Lab software and normalized to the levels of β-tubulin or Gapdh, which acted as loading controls.

Antibodies

Primary antibodies specific for the following proteins were obtained from Cell Signaling Technology: LC3B (#3868), p62 (#39,749), SCD1 (#2794), Fas (#3180), mTOR (#2983), p-mTOR (#5586), p70S6k (#2708), p-p70S6k (#9234), Ampkα (#58,313), and p-Ampkα (#50,081). Additionally, a primary antibody to HGF (26,881–1-AP), EEA1 (68,065–1-Ig), Rab11a (67,902–1-Ig), Rab5a (66,339–1-Ig), Rab7a (55,469–1-AP), and LAMP1 (67,300–1-Ig) were purchased from Proteintech. Primary antibodies to Srebp1 (abs131802), β-tubulin (abs171597), and Gapdh (abs173393) were purchased from absin. In Western Blotting experiments, secondary antibodies goat anti-rabbit-IgG (#abs20040) and goat anti-mouse-IgG (#abs20039) from absin were utilized to detect primary antibody-bound target proteins. For Immunofluorescence analysis, CoraLite488-conjugated Goat Anti-Rabbit IgG (#SA00013-2) and CoraLite594-conjugated Goat Anti-Rabbit IgG (#SA00013-4) secondary antibodies were used, both sourced from Proteintech.

Coculturing of cells

The hepatocytes (human HepG2 cells and mouse AML12 cells) were cultured in Transwell chambers with a 24 mm diameter and 0.4 mm pore size from Corning. A total number of 5×10^5 cells were seeded in the lower chamber in DMEM medium. The MSC^{shGfp} or MSC^{shAtg5} cells (1×10^5 cells) were seeded into the upper chamber in the same medium. After 24 h of co-culture, FFAs were added to the co-culture system. The hepatocytes were then harvested after another 24 h for Nile Red staining, TGs detection, qPCR analysis, or Western blotting.

Cell cycle assay

The MSC^{shGfp} or MSC^{shAtg5} cells were seeded at a density of 2×10^5 cells per 25 cm^2 cell culture dish. After 12 h of seeding, the cells were washed three times with 10 ml of PBS. Subsequently, FFAs were added as per the experimental requirements. The cells were then fixed with 70% ethyl alcohol and stained with the Cell Cycle Detection Kit (C-1052, Beyotime, China). Cell cycle analyses were conducted using a BD FACS flow cytometer, and the resulting data were analyzed using FlowJo software.

Cell apoptosis assay

The MSC^{shGfp} or MSC^{shAtg5} cells were cultured in a 25 cm^2 cell culture dish and pre-treated with FFAs for 24 h. Apoptotic cells were then identified using FITC-Annexin V and propidium iodide (C1062L, Beyotime China) for 30-min incubation at room temperature. The number of

apoptotic cells was determined using a BD FACS flow cytometer, and the resulting data were analyzed using FlowJo software.

Histological Analyses

Histological analysis was conducted following the methodology described in a previous report [6]. For H&E staining, paraformaldehyde (PFA)-fixed, paraffin-embedded liver tissue was sectioned into 5 μm slices and stained with H&E to observe the pattern of liver morphology. For Oil Red O staining, the sections were initially fixed in 60% isopropanol for 10 min, then stained with a freshly prepared Oil Red O working solution for 30 min, followed by washing with 60% isopropanol. Subsequently, the sections were counterstained with hematoxylin, washed with 4% acetic acid solution, and finally mounted with an aqueous solution.

Induction of senescence

The MSC^{shGfp} or MSC^{shAtg5} cells were seeded onto 12-well plates at a density of 1×10^4 cells per well. After an overnight incubation, the MSCs were treated with 400 μM FFAs. Following this treatment, the media was replaced with fresh DMEM, and the cells were cultured for an additional 3 days. Subsequently, in situ staining for senescence-associated β-galactosidase (SA-β-gal) was performed on the cells using a senescence β-galactosidase staining kit (C0602, Beyotime) following the manufacturer's instructions. The presence of cytoplasmic staining was used to determine positivity for SA-β-gal staining in the cells. Quantification of the total number of β-gal + cells was performed in ten high-power fields.

EdU cell proliferation

The MSC^{shGfp} or MSC^{shAtg5} cells were seeded in 12-well plates at a density of 1×10^4 cells per well. The cells were pre-treated with 400 μM FFAs and then stained with BeyoClick EdU-555 (C0075S, Beyotime China) for 2 h, following the manufacturer's instructions. Fluorescence was detected and measured using fluorescent microscopy. Quantification of the total number of CD68 + cells was performed in seven high-power fields.

Nile red staining

The cells were exposed to 400 μM FFAs for 24 h. Following the treatment, the cells were fixed with 4% PFA and stained with Nile red (sigma) in a dark environment at room temperature for 15 min. DAPI staining was then conducted to visualize the nuclei. Images of the stained cells were captured using confocal laser scanning microscopy.

Murine serological analysis

Blood glucose levels were monitored using a Sinocare automatic glucometer. Glucose tolerance tests (GTTs) were conducted by administering an intraperitoneal injection (i.p.) of glucose (2 g/kg) to mice following a 16-h fasting period. Insulin tolerance tests (ITTs) were performed by injecting insulin (0.75 U/kg) i.p. after a 6-h fasting period. Blood glucose samples were collected from the tail vein and analyzed at specific time points (15, 30, 60, and 90 min).

Serum enzymes including alanine aminotransferase (ALT) and aspartate aminotransferase (AST) levels were determined using specific assay kits (C009/C010, Nanjing Jiancheng, China) according to the manufacturer's instructions. Additionally, the levels of serum and hepatic triglycerides (TG) were measured using commercial kits (A110, Nanjing Jiancheng, China) following the manufacturer's guidelines.

Immunofluorescence

For immunofluorescence (IF) analysis, cells were fixed with 4% PFA. After blocking and permeabilization, the cells were incubated with primary antibodies and then with Fluorescein-conjugated secondary antibodies. Nuclei were counterstained with DAPI. Images were captured using a confocal laser scanning microscope to visualize the localization and expression of the target proteins within the cells.

Elisa assays

The ELISA assay was used to analyze the cytokine levels in the conditioned medium of MSC^{shgfp} or MSC^{shAtg5}. After culturing for 24, 48, and 72 h, the conditioned medium was collected and concentrated tenfold using ultrafiltration. Subsequently, based on the antibody microarray data, paracrine cytokines in the culture medium were analyzed using the human Angiogenin/VEGF/HGF/bFGF and Ang-2 ELISA kit (Boster, China) following the manufacturer's guidelines.

Statistical analysis

All experiments were repeated at least three times independently. Statistical analysis was conducted using GraphPad Prism software. For comparisons among multiple groups, one-way ANOVAs followed by the Tukey test were employed. Two-way ANOVA was utilized for statistical analysis in the GTTs ITTs. Pairwise comparisons were performed using the unpaired Student's t-test. All quantitative data are expressed as mean values ± SEM. Significance levels were set at $P<0.05$, with the following categorization for *P*-values: $^{*}P<0.05$, $^{**}P<0.005$, $^{***}P<0.001$.

Results

Atg5-deficient MSCs displayed higher cell proliferation, resistance to cellular senescence, and apoptosis under FFAs treatment

To assess the biological characteristics of autophagy-deficient MSCs, we employed lentiviral transduction to silence Atg5 in human adipose-derived MSCs, creating MSC^{shAtg5} [18]. This manipulation significantly reduced both Atg5 mRNA and protein expression levels (Fig. 1A, B). Nevertheless, MSC^{shAtg5} demonstrated a slight increase in proliferation and cell viability as determined by the CCK-8 assay (Fig. 1C).

Given the commonly elevated blood lipid levels in NAFLD disease models and the potential disruption of MSC functions by these elevated lipids [19], we investigated the effects of FFAs on MSC functions in both MSC^{shAtg5} and wild-type MSCs. Following 24 h of 400 μM FFAs treatment, MSCs demonstrated significantly suppressed proliferation with evident signs of cell senescence. In contrast, MSC^{shAtg5} exhibited improved cell proliferation and reduced senescence, as confirmed by 5-Ethynyl-2'-deoxyuridine (EdU) and β-galactosidase (βgal) staining (Fig. 1D, E). Additionally, flow cytometry analysis revealed a shift in the cell cycle from G0/G1 phase and S phase to G2/M phase in MSC^{shAtg5} (Fig. 1F). Furthermore, MSC^{shAtg5} showed slightly increased resistance to FFA-induced apoptosis (Fig. 1G). Overall, these results indicated that Atg5 deficiency can enhance MSCs functionalities with more resistance to senescence and apoptosis under FFAs treatment.

Atg5-deficient MSCs inhibit lipid accumulation in hepatocytes

Previous studies have suggested that adipose-derived MSCs may offer benefits in improving NAFLD [20]. To further explore the potential impacts of Atg5-deficient MSCs on NAFLD improvement, we conducted a co-culture system with MSCs and hepatocytes to assess the role of MSCs in modulating lipid metabolism. Our results demonstrate that MSC^{shAtg5} can significantly reduce the lipid content in liver cells induced by FFAs processing, as evidenced by Nile red staining and a triglycerides (TGs) detection test (Fig. 2A, B). Additionally, we examined the expression of lipid synthesis-related genes (*Fas*, *Srebp1*, and *SCD1*) at both the RNA and protein levels. It was observed that FFAs stimulation significantly increased the expression of these genes. However, compared to control MSCs, MSC^{shAtg5} exhibited a more substantial decrease in the expression of these genes (Fig. 2C-F). These findings suggest that Atg5-deficient MSCs may have a more pronounced effect in reducing lipid accumulation in liver cells in vitro.

Atg5-deficient MSCs transplantation attenuates NAFLD-related metabolic disorders

To further investigate the effects of Atg5-deficient MSCs transplantation on lipid metabolism, we utilized a mouse model of HFD-induced fatty liver to assess the therapeutic potential of MSCs. As previously mentioned, the transplantation strategy is illustrated in Fig. 3A [6]. Whether mice received transplantation of control MSCs or Atg5-deficient MSCs, there appeared to be no effect on their food intake (Fig. 3B). After 16 weeks of a HFD regimen, mice exhibited significant increases in liver/body weight ratio, fasting blood glucose, and fasting insulin levels. The transplantation of MSCs effectively reduced these markers (Fig. 3C-E). However, compared to control MSCs, MSC^{shAtg5} transplantation showed a more pronounced decrease in the liver/body weight ratio and fasting blood glucose levels (Fig. 3C, D). We further investigated the protective effect of MSCs on liver function. Our results demonstrated that MSC^{shAtg5} transplantation led to a more substantial decrease in alanine aminotransferase (ALT) and aspartate aminotransferase (AST) levels in the serum of HFD-fed mice compared to control MSCs (Fig. 3F). Glucose tolerance tests (GTTs) and insulin tolerance tests (ITTs) revealed that insulin resistance was significantly restored with MSC^{shAtg5} transplantation compared to unmodified MSCs (Fig. 3G). These findings suggest that Atg5-deficient MSCs have a greater capacity to improve HFD-induced liver dysfunction and insulin resistance.

Biochemical and histological analyses revealed a significant increase in serum and hepatic TGs in mice fed a HFD compared to those fed a normal chow diet (NCD) (Fig. 3I, J). Transplantation of MSCs significantly improves the morphology of liver tissue and reduces hepatic lipid accumulation in HFD-fed mice, as indicated by HE and Oil Red O staining (Fig. 3H). Importantly, transplantation of MSC^{shAtg5} demonstrates a superior effect in reducing hepatic fat accumulation (Fig. 3H-J). Moreover, we found MSC^{shAtg5} resulted in a more significant inhibition of the expression of genes (*Fas*, *Srebp1*, and *SCD1*) involved in fatty acid synthesis and, which was notable in the presence of long term HFD treatment, at the transcriptional and translational levels (Fig. 3K, L). In addition, transplantation of MSC^{shAtg5} can significantly suppress the expression of inflammation-related genes (*Tnf*, *Il6*, and *Ccl2*) at the transcriptional level compared to control MSCs (Fig. 3K). These data suggest that Atg5-deficient MSCs have a better effect in inhibiting lipid accumulation and suppressing inflammatory responses.

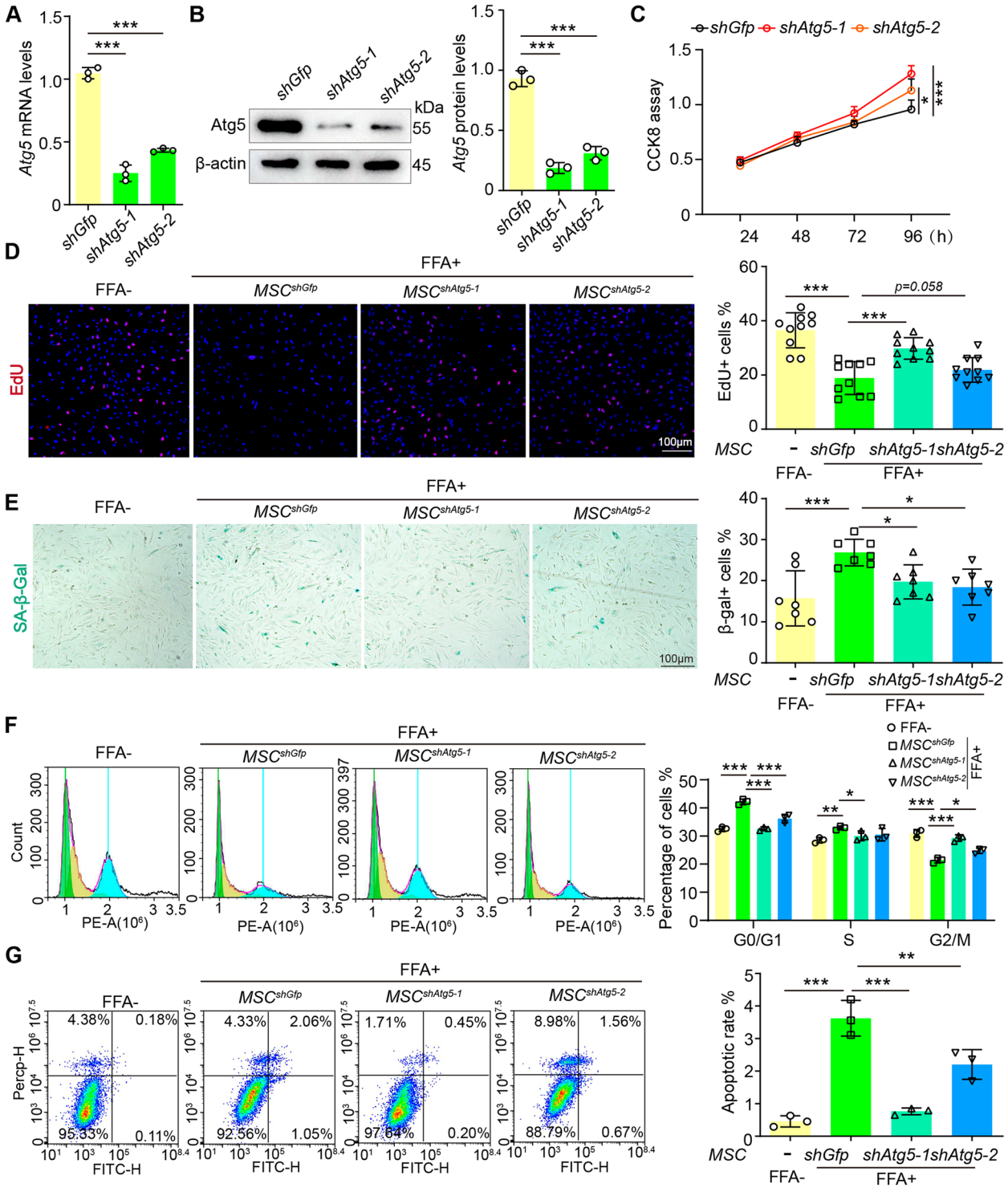

Fig. 1 Atg5-deficient MSCs exhibited increased cell proliferation, resistance to cellular senescence, and reduced apoptosis under FFAs treatment. **A**, **B** *Atg5* mRNA and protein expression in MSCs transfected with lentivirus containing Atg5 shRNA. **C** CCK8 assays comparing MSC^{shGfp} and MSC^{shAtg5}. **D** EdU staining of MSC^{shGfp} and MSC^{shAtg5} was performed after a 24-h treatment with FFAs, with representative micrographs shown and scale bars of 100 μm. **E** In situ staining of SA-β-gal was conducted using a senescence β-galactosidase staining kit, with representative micrographs and 100 μm scale bars. **F** Cell cycle analysis of MSC^{shGfp}, presented for the G0/G1, S, and G2/M phases under various treatment conditions. **G** Cell apoptosis analysis was performed in the indicated groups. All statistical analyses are presented on the right panel of data. For all statistical plots, the data are presented as mean ± S.E.M, and statistical significance is indicated as $^{*}P < 0.05$, $^{**}P < 0.01$, $^{***}P < 0.001$. MSCs, mesenchymal stem cells; FFAs, free fatty acids; EdU, 5-Ethynyl-2′-deoxyuridine; SA-β-gal, Senescence-associated β-galactosidase

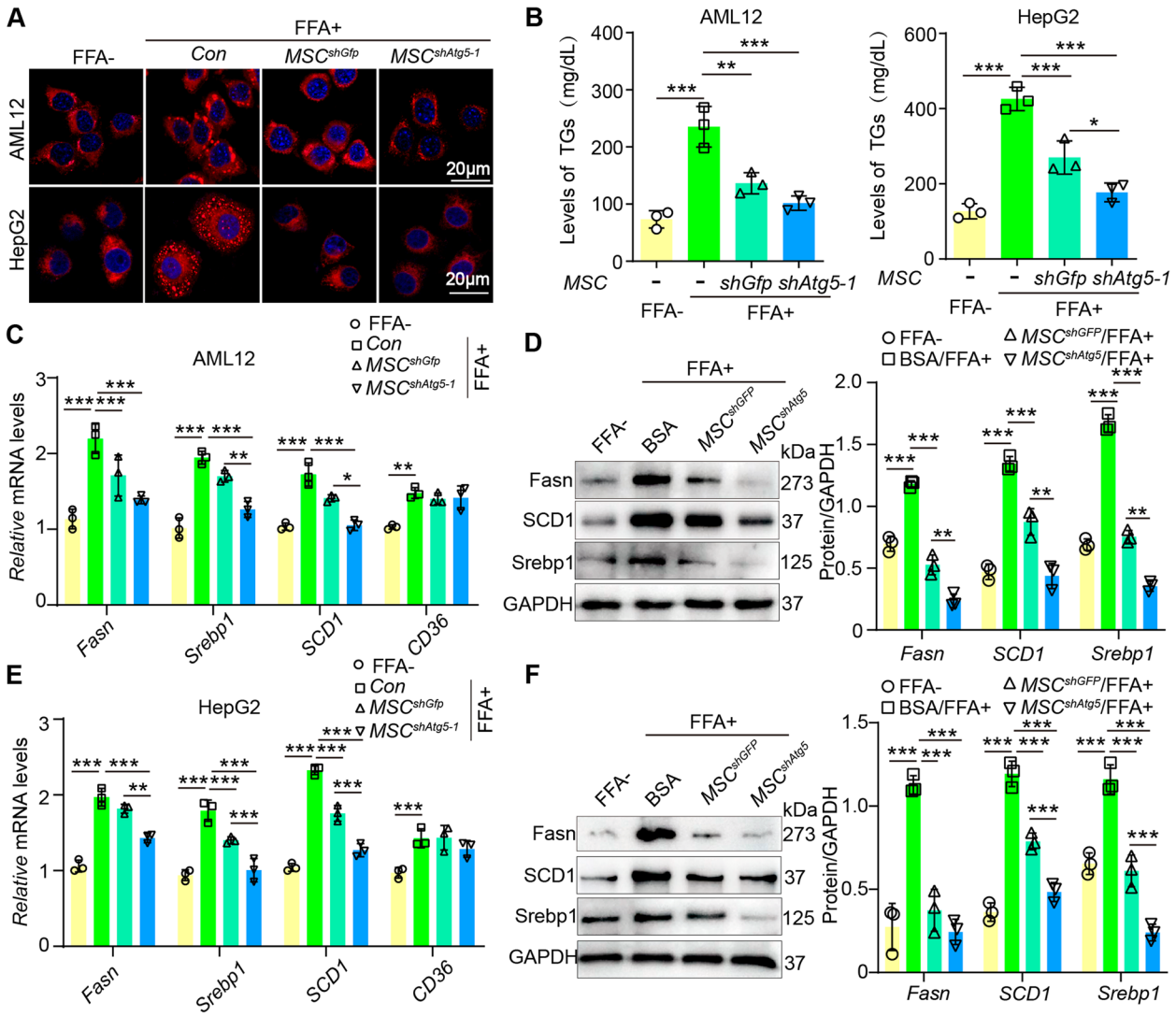

Fig. 2 Atg5-deficient MSCs inhibit lipid accumulation in hepatocytes. **A** Representative images of Nile Red staining in hepatocytes cocultured with MSC^{shGfp} and MSC^{shAtg5} following FFAs treatment. Scale bar = 20 μm. **B** The levels of TGs in the indicated groups. **C**, **E** qPCR analysis of lipid metabolism-related genes (*Fasn, Srebp1, SCD1* and *CD36*) in the indicated groups. **D**, **F** Western blot of lipid metabolism related proteins in the indicated groups. For all statistical plots, the data are presented as mean ± S.E.M, and statistical significance is indicated as $^{*}P < 0.05$, $^{**}P < 0.01$, $^{***}P < 0.001$. MSCs, mesenchymal stem cells; TGs, triglycerides

Atg5-deficient MSCs correct AMPKα/mTOR/S6K/Srebp1 signaling in NAFLD disease models

Excessive lipid deposition disrupts metabolic pathways and accelerates the progression of NAFLD. Dysregulation of the mTOR pathway, a key regulator of cellular processes including protein synthesis and metabolism, has been implicated in the development of metabolic disorders such as obesity and fatty liver diseases [21]. Several studies have demonstrated that mTOR regulates downstream p-70S6K to promote the cleavage and activation of SREBPs to regulate fatty acid metabolism [22]. Moreover, AMPK is a key cellular energy sensor that functions as an endogenous inhibitor of the mTOR pathway [23]. In the context of NAFLD, aberrant inactivation of AMPK or activation of mTOR signaling can promote lipid accumulation and hepatic steatosis [24].

To verify the effects of MSCs transplantation on lipid metabolism-related pathways, we collected hepatocytes co-cultured with MSCs in vitro and liver tissues after MSCs transplantation in vivo to perform western blotting tests. The results show that in both mouse and cell models of NAFLD, there was a reduction in the expression

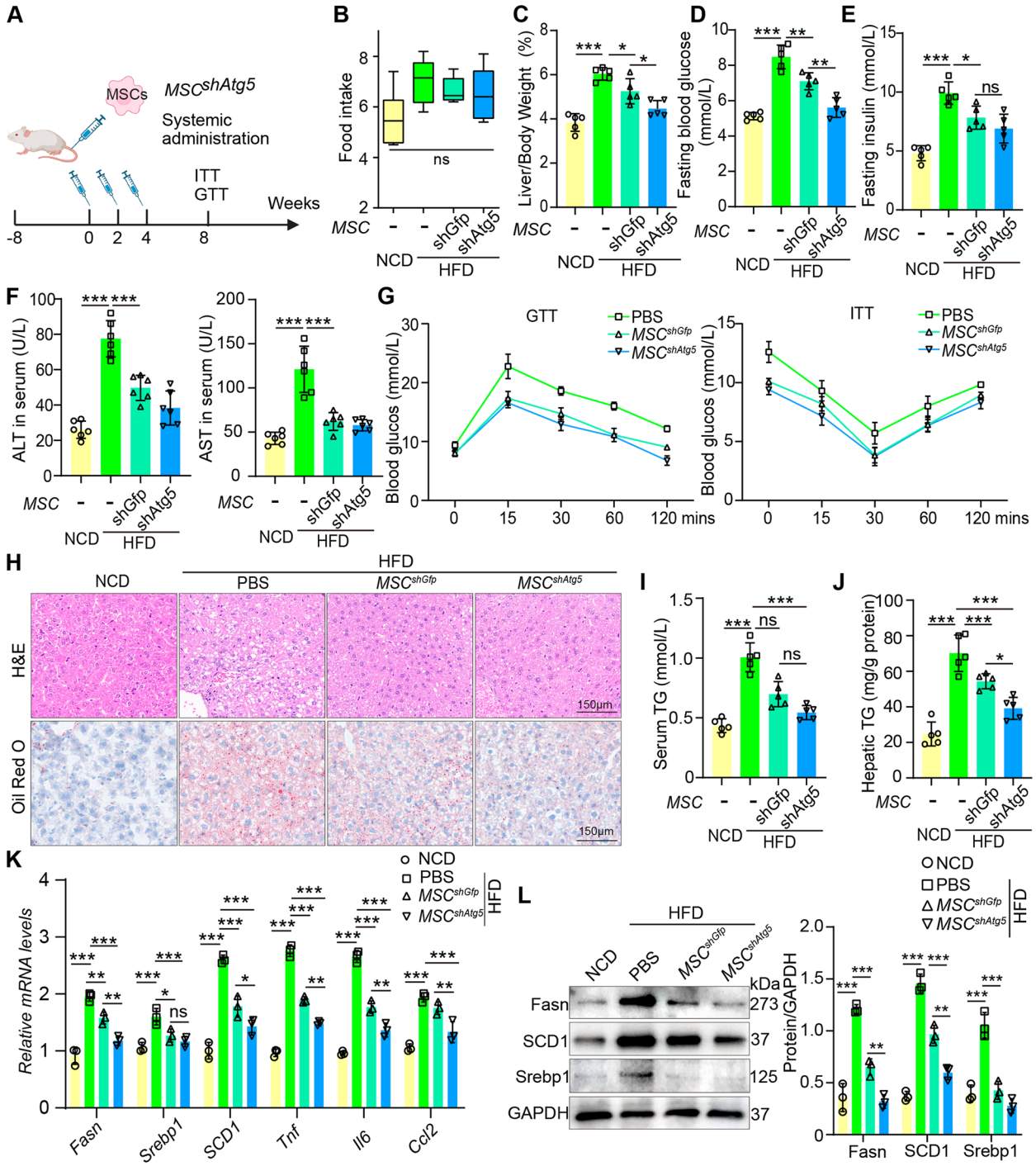

Fig. 3 Transplantation of Atg5-deficient MSCs attenuates NAFLD-related metabolic disorders. **A** Schematic protocol for administration of PBS, MSC^{shGfp} and MSC^{shAtg5} into NCD or HFD mice. **B**, **C** Statistical data on food intake and the liver-to-body weight ratio in the indicated groups. **D**, **E** Analysis of fasting blood glucose and fasting insulin levels in the mice. **F** Serum levels of ALT and AST in the indicated groups. **G** Analysis of GTTs and ITTs in the indicated groups ($n = 5$). **H** Representative HE and Oil Red O staining of liver sections from MSC^{shGfp} and MSC^{shAtg5} transplated mice after HFD treatment ($n = 5$). Scale bar = 150 μm. **I**, **J** Levels of TGs in the serum and liver of mice. **K** qPCR analysis of lipid metabolism-related genes (*Fasn*, *Srebp1*, and *SCD1*) and inflammation-related genes (*Tnfa*, *Il6*, and *Ccl2*) in the indicated groups. **L** Western blot analysis of lipid metabolism-related proteins in the indicated groups. For all statistical plots, circles represent individual mice, the data are presented as mean ± S.E.M, and statistical significance is indicated as ns means not significant, *$P < 0.05$, **$P < 0.01$, ***$P < 0.001$. MSCs, mesenchymal stem cells; NAFLD, non-alcoholic fatty liver disease; NCD, normal chow diet; HFD, high-fat diet; TGs, triglycerides; ALT, alanine aminotransferase; AST, aspartate aminotransferase; GTTs, Glucose tolerance tests, ITTs: insulin tolerance tests

levels of p-AMPKα, accompanied by an increase in the expression levels of p-mTOR, p-S6K, and Srebp1. However, following co-cultivation or tail vein transplantation of MSC^{shGfp}, there was an increase in the expression levels of p-AMPKα in hepatocytes and livers, along with a decrease in the expression levels of p-mTOR, p-S6K, and Srebp1. The changes in expression patterns were more pronounced following co-cultivation or transplantation of MSC^{shAtg5} (Fig. 4A-F). These results indicate that the regulation of the AMPKα/mTOR/S6K/Srebp1 pathways by MSCs, particularly Atg5-deficient MSCs, could potentially have a beneficial impact on mitigating NAFLD.

The deficiency of Atg5 enhances the secretion of HGF by promoting recycling endosome production in MSCs

Increasing evidence suggests that MSCs exert their beneficial effects in improving diseases through the releasing paracrine cytokines [25–27]. Here, we identified specific cytokines secreted by human adipose-derived MSCs, noting a significant abundance of Angiogenin, VEGF, HGF, and bFGF in their conditioned medium (Fig. 5A). Upon comparing levels of these factors in MSC^{shGfp} and MSC^{shAtg5}, we observed a substantial increase solely in HGF secretion from Atg5-deficient MSCs (Fig. 5B). Furthermore, our investigation revealed that MSC^{shAtg5} consistently enhanced the secretion of HGF over varying culture durations, implying that Atg5 deficiency amplifies HGF secretion by MSCs (Fig. 5C).

Subsequently, we observed a significant inhibition of autophagic activity in MSC^{shAtg5}, as evidenced by the upregulation of LC3II and downregulation of p62. Moreover, both mRNA and protein levels of HGF increased in MSC^{shAtg5} (Fig. 5D, E). To further investigate the role of autophagy in regulating HGF expression, we utilized 3-methyladenine (3-MA) to block autophagosome synthesis. Strikingly, HGF expression in both MSC^{shGfp} and MSC^{shAtg5} was upregulated following 3-MA treatment. In contrast, treatment of MSCs with the lysosomal inhibitor chloroquine (CQ) did not result in a promotion of HGF expression (Fig. 5F). These findings suggest that the expression of HGF is influenced by early autophagy events, particularly during the autophagosome formation stage, rather than the lysosomal stage.

Previous reports have indicated that various membranes, including recycling endosomes (REs), play a role in the formation of autophagosomes [28]. This suggests that maintaining cellular homeostasis requires a balance between autophagosomes and endosomes [29]. Different Rab proteins are expressed in early endosomes (EEs), late endosomes (LEs), and REs, participating in virtually every membrane trafficking event [30]. In our study, we utilized immunofluorescence to examine the expression and distribution of the Rab5a (EEs), Rab11a (REs), LAMP1 (lysosomes) and HGF. Our results indicated a decrease in both the number of EEs and lysosomes, while the expression of REs increased (Fig. 5G-I). Western blot analysis further revealed decreased levels of Rab5a and EEA1, as well as reduced expression of Rab7a and LAMP1 in MSC^{shAtg5}. In contrast, the expression of the REs marker Rab11a and HGF were increased (Fig. 5J). Furthermore, in cells with autophagy defects, immunofluorescence staining of Rab11 is more prominently expressed on the cell membrane, providing further evidence that the sorting of REs is enhanced (Fig. 5H). These findings suggest that Atg5 deficiency may enhance the secretion of HGF by increasing the number of intracellular REs.

The protective effect of Atg5-deficient MSCs on NAFLD lipid metabolism disorder depends on the secretion of HGF

Atg5 deficiency promotes MSC secretion of HGF to protect against NAFLD. To further confirm the crucial role of HGF in MSC^{shAtg5}-mediated protection against NAFLD, we generated MSCs with dual genetic defects in Atg5 and HGF ($MSC^{shAtg5/HGF}$). The results indicate that transplantation of MSCs modified with different genes does not impact food intake and body weight changes (Fig. 6A, B). However, compared to MSC^{shAtg5}, transplantation of $MSC^{shAtg5/HGF}$ increases the liver/body weight ratio, fasting blood glucose, and fasting insulin levels (Fig. 6C-E). Furthermore, results from GTTs and ITTs demonstrate that transplantation of MSCs with dual gene defects worsens insulin resistance, a benefit that is improved by MSC^{shAtg5} transplantation (Fig. 6F). Additionally, liver aminotransferase experiments reveal that levels of ALT and AST in the serum of $MSC^{shAtg5/HGF}$ transplantation are higher compared to MSC^{shAtg5} (Fig. 6G). These findings suggest that the improved liver dysfunction and insulin resistance in HFD-induced mice

(See figure on next page.)

Fig. 4 Atg5-deficient MSCs correct AMPKα/mTOR/S6K/Srebp1 signaling in NAFLD disease models. **A**, **B** Western blot analysis of p-AMPKα/AMPKα, p-mTOR/mTOR, p-S6K/S6K, and Srebp1 in AML12 cells cocultured with MSC^{shGfp} and MSC^{shAtg5} following FFAs treatment. **C**, **D** Western blot analysis in HepG2 cells cocultured with different MSCs. **E**, **F** Western blot analysis of p-AMPKα/AMPKα, p-mTOR/mTOR, p-S6K/S6K, and Srebp1 in HFD mice receiving different MSC transplantations. For all statistical plots, the data are presented as mean ± S.E.M, and statistical significance is indicated as $^{*}P < 0.05$, $^{**}P < 0.01$, $^{***}P < 0.001$. MSCs, mesenchymal stem cells; NAFLD, non-alcoholic fatty liver disease; FFAs, free fatty acids; HFD, high-fat diet

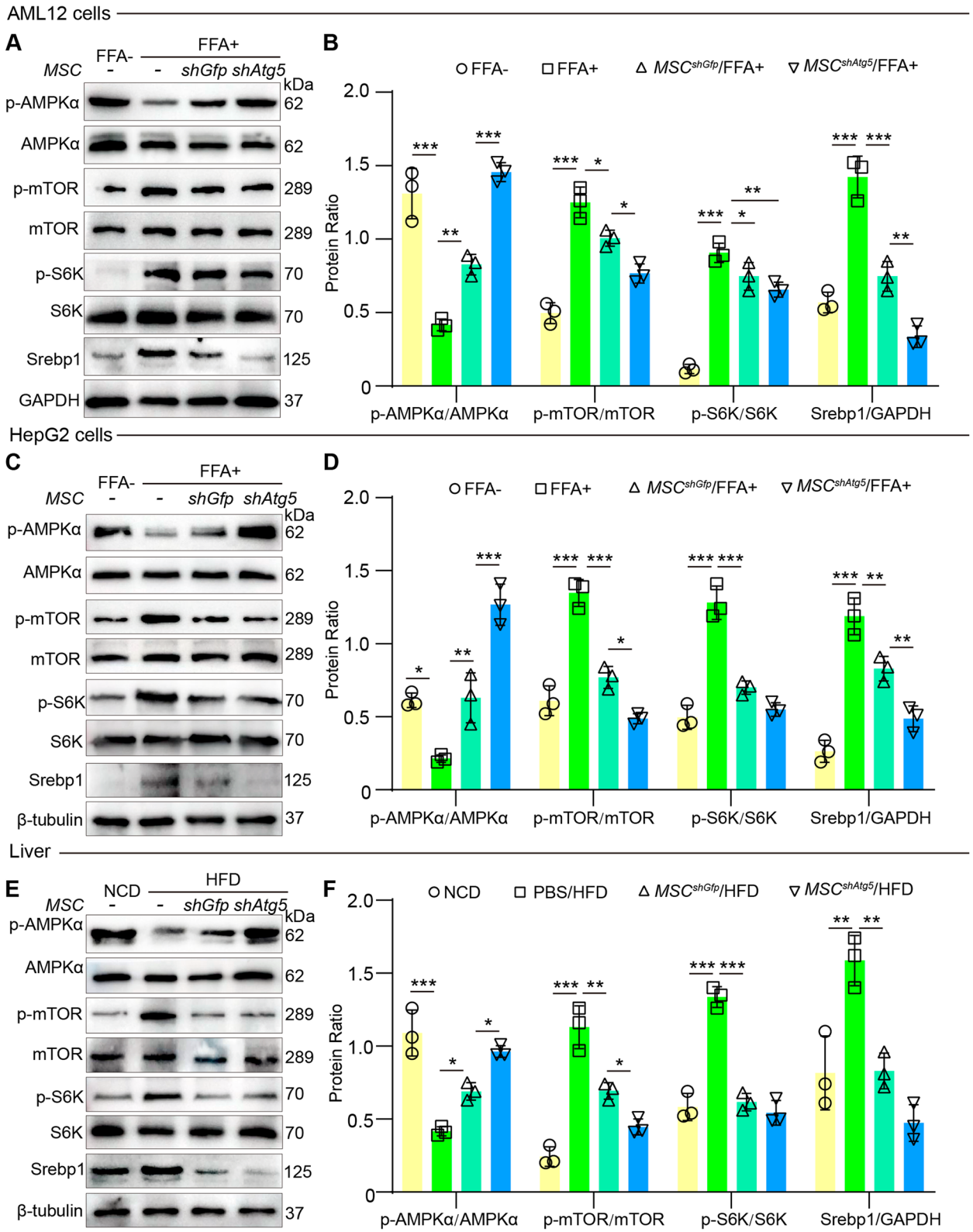

Fig. 4 (See legend on previous page.)

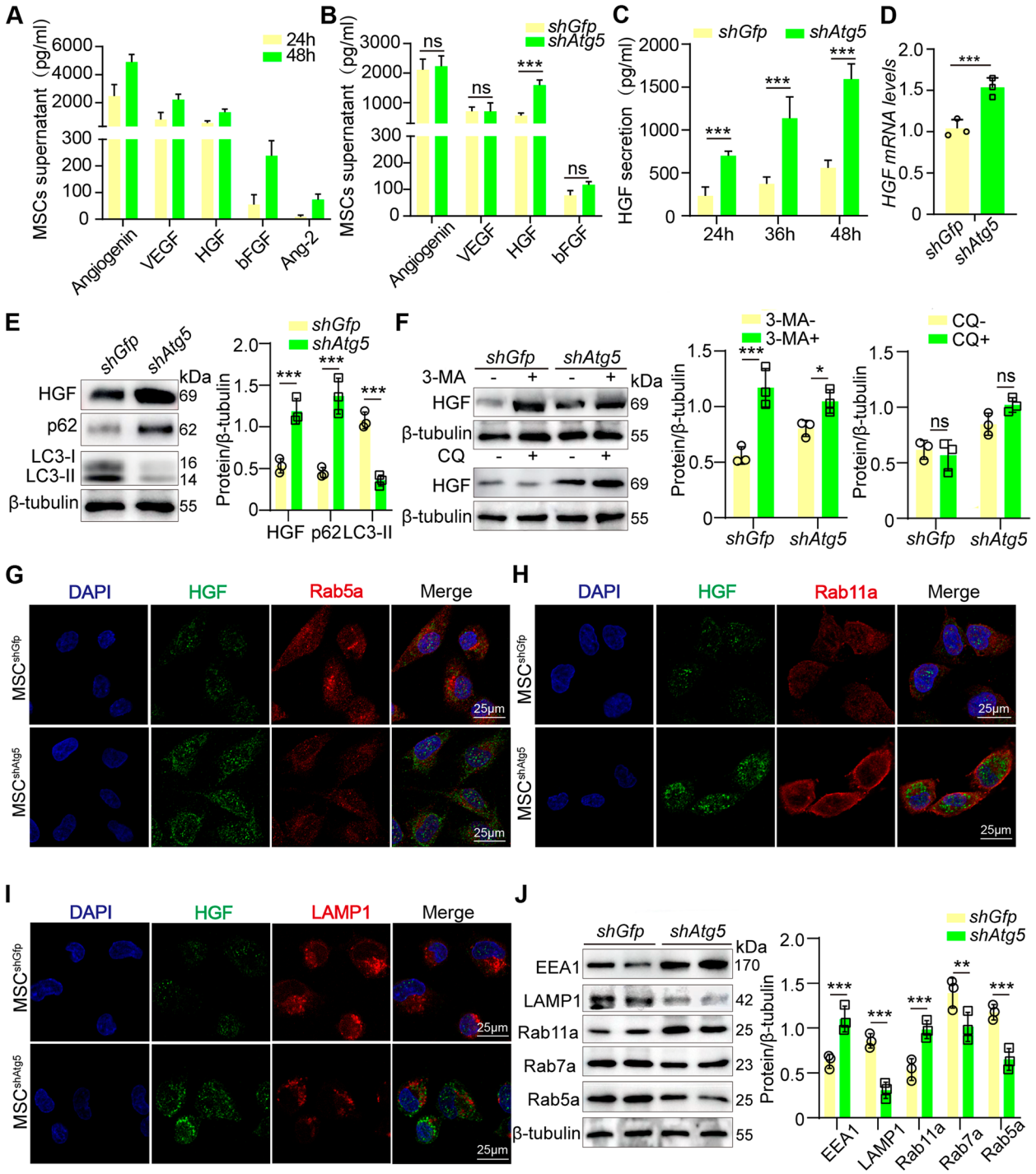

Fig. 5 The deficiency of Atg5 enhances the secretion of HGF by promoting RE production in MSCs. **A** ELISA detection of various growth factors in the MSC supernatant, including Angiogenin, VEGF, HGF, bFGF, and Ang-2. **B** ELISA detection of the secretion of different factors in the supernatants of MSC^{shGfp} and MSC^{shAtg5}. **C** ELISA detection of HGF secretion at different culture times in MSC^{shGfp} and MSC^{shAtg5}. **D** qPCR analysis of HGF transcription in MSC^{shGfp} and MSC^{shAtg5}. **E** Western blot analysis of the expression of HGF, P62, and LC3 in MSC^{shGfp} and MSC^{shAtg5}. **F** MSC^{shGfp} and MSC^{shAtg5} treated with 3-MA and CQ, followed by Western blot detection of HGF expression. **G-I** Representative images of immunofluorescence staining analyzing the expression of Rab5a, Rab11a, LAMP1, and HGF. Scale bar = 25 μm. **J** Western blot analysis of the expression of endosome sorting-related proteins (EEA1, Rab11a, Rab5a, Rab7a, and LAMP1). For all panels, the data are presented as mean ± S.E.M, and statistical significance is indicated as $^{*}P < 0.05$, $^{**}P < 0.01$, $^{***}P < 0.001$. ELISA, Enzyme linked immunosorbent assay; HGF, hepatocyte growth factor; RE, recycling endosome; 3-MA, 3-methyladenine; CQ, chloroquine

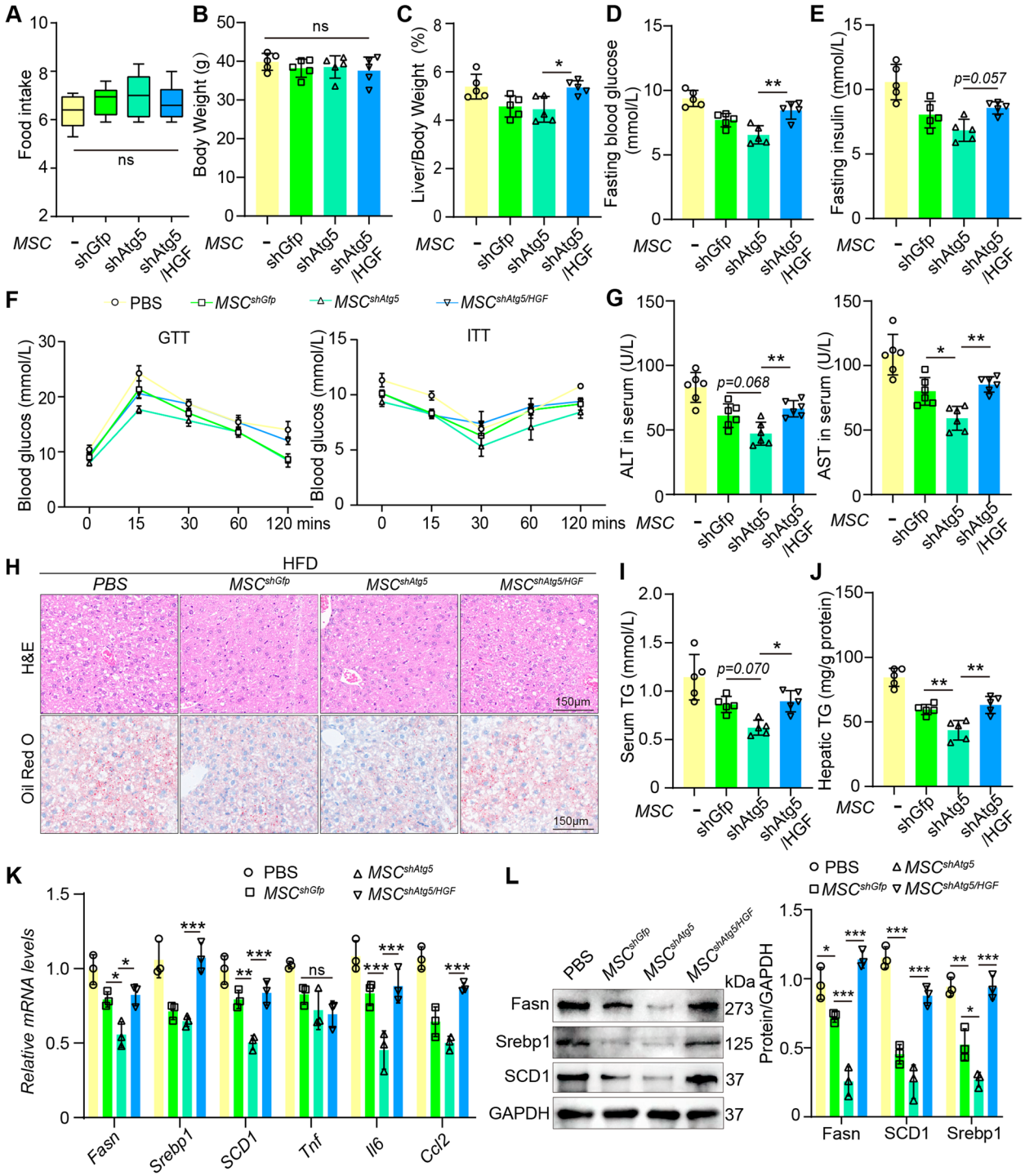

Fig. 6 The protective effect of Atg5-deficient MSCs on NAFLD lipid metabolism disorder depends on the secretion of HGF. **A-C** Statistical data on food intake, body weight and the liver-to-body weight ratio in the indicated groups. **D**, **E** Analysis of fasting blood glucose and fasting insulin levels in the mice. **F** Analysis of GTTs and ITTs in the PBS, MSC^{shGfp}, MSC^{shAtg5} and $MSC^{shAtg5/HGF}$ treated mice ($n=5$). **G** Serum levels of ALT and AST in the indicated groups. **H** Representative HE and Oil Red O staining of liver sections from the MSC^{shGfp}, MSC^{shAtg5} and $MSC^{shAtg5/HGF}$ transplated mice after HFD treatment ($n=5$). Scale bar = 150 μm. **I**, **J** Levels of TGs in the serum and liver of mice. **K** qPCR analysis of lipid metabolism-related genes (*Fasn, Srebp1,* and *SCD1*) and inflammation-related genes (*Tnfa, Il6,* and *Ccl2*) in the indicated groups. **L** Western blot analysis of lipid metabolism-related proteins in the indicated groups. For all statistical plots, circles represent individual mice, the data are presented as mean ± S.E.M, and statistical significance is indicated as ns means not significant, $^{*}P<0.05$, $^{**}P<0.01$, $^{***}P<0.001$. MSCs, mesenchymal stem cells; NAFLD, non-alcoholic fatty liver disease; HFD, high-fat diet; TGs, triglycerides; ALT, alanine aminotransferase; AST, aspartate aminotransferase; GTTs, Glucose tolerance tests, ITTs: insulin tolerance tests

by MSC^{shAtg5} transplantation is compromised in the absence of HGF.

As previously reported, the transplantation of MSC^{shAtg5} significantly reduces lipid accumulation in NAFLD mice. However, symptoms of lipid accumulation were notably exacerbated following the transplantation of $MSC^{shAtg5/HGF}$ compared to MSC^{shAtg5} transplantation, as demonstrated by biochemical and histological analyses (Fig. 6H-J). Furthermore, at the molecular level, we observed that MSC^{shAtg5} transplantation significantly decreased the expression levels of factors associated with lipid synthesis and inflammation. In contrast, the expression levels of lipid synthesis and inflammatory factors increased following the transplantation of $MSC^{shAtg5/HGF}$ (Fig. 6K, L). These findings suggest that the protective effect of Atg5-deficient MSCs on liver lipid accumulation in NAFLD mice relies on the secretion of HGF.

3-MA-primed MSCs protect against NAFLD through enhancing HGF secretion

Based on our previous findings, inhibition of autophagosome formation affects the secretion of hepatocyte growth factor (HGF) from MSCs, while inhibiting the fusion between autophagosomes and lysosomes does not impact HGF secretion. Therefore, to further investigate the role of MSCs with inhibited autophagosome formation in the treatment of NAFLD, we conducted experiments in which MSCs were pretreated with 3-methyladenine (3-MA). As expected, the 3-MA-primed MSCs exhibited autophagy-inhibiting properties, as indicated by the expression levels of LC3 and P62 proteins (Fig. 7H). Transplantation of these 3-MA-primed MSCs significantly reduced fasting blood glucose and insulin levels in NAFLD mice compared to control MSCs (Fig. 7A, B). Additionally, these pre-treated MSCs decreased serum levels of ALT and AST in mice on a HFD (Fig. 7C, D). GTTs and ITTs showed that the transplantation of 3-MA-treated MSCs significantly improved insulin sensitivity relative to control MSCs (Fig. 7E). Furthermore, these MSCs reduced hepatic lipid accumulation in HFD mice, as evidenced by HE staining, Oil Red O staining, and serum and hepatic TGs levels (Fig. 7F, G). At the molecular level, 3-MA-primed MSCs inhibited the expression of lipogenic factors such as Fasn, Srebp1, and SCD1, while reducing phosphorylated mTOR levels and enhancing phosphorylated AMPKα expression (Fig. 7I). These findings suggest that the transplantation of 3-MA-primed MSCs regulates lipid metabolic disorders in NAFLD through the AMPKα-mTOR signaling pathway.

Through WB and ELISA assays, we found that the protein levels and secretion of HGF were significantly enhanced in 3-MA-treated MSCs, consistent with the results observed in MSCs with Atg5 deficiency (Fig. 7H, J). Furthermore, we discovered that the recycling endosome marker Rab11a was upregulated in 3-MA-primed MSCs, as analyzed by WB and immunofluorescence experiments (Fig. 7I, K). These findings indicate that 3-MA-primed MSCs promote HGF secretion by enhancing recycling endosome sorting. Furthermore, qPCR analysis revealed that the co-culture of HGF-deficient cells pre-treated with 3-MA significantly increased the expression of lipid synthesis genes and inflammation-related factors compared to 3-MA-primed MSC^{shGfp} (Fig. 7L). These findings indicate that 3-MA-primed MSCs inhibit the inflammatory response and lipid accumulation in the NAFLD hepatocyte model through HGF secretion.

Discussion

Mesenchymal stem cells (MSCs) exert therapeutic effects on various diseases through the secretion of numerous factors and immune regulation. In recent years, gene knockdown and overexpression techniques have been utilized to genetically modify MSCs, thereby enhancing the expression of various factors and increasing the production of therapeutic metabolites to improve disease outcomes [31]. Autophagy is a crucial process for maintaining the balance of proteins and metabolic products within the body [3]. In this study,

(See figure on next page.)

Fig. 7 3-MA-primed MSCs protect against NAFLD through enhancing HGF secretion. **A**, **B** Analysis of fasting blood glucose and fasting insulin levels in the serum of mice treated with MSCs and 3-MA primed MSCs. **C**, **D** Serum levels of ALT and AST in the indicated groups. **E** Analysis of GTTs and ITTs in the MSCs and 3-MA primed MSCs treated mice ($n = 5$). **F** Representative HE and Oil Red O staining of liver sections in the indicated groups ($n = 5$). Scale bar = 150 μm. **G** Levels of TGs in the serum and liver of mice. **H** Western blot analysis of the expression of HGF, P62, and LC3 in MSCs and 3-MA primed MSCs. **I** ELISA detection of HGF secretion at different culture times in MSCs and 3-MA primed MSCs. **J** Representative images of immunofluorescence staining analyzing the expression of Rab11a and HGF. **K** Western blot analysis of p-AMPKα/AMPKα, p-mTOR/mTOR, Fasn, Srebp1, SCD1 and Rab11a in HFD mice receiving different MSC transplantations. Scale bar = 25 μm. **L** qPCR analysis of lipid metabolism-related genes (*Fasn, Srebp1* and *SCD1*) and inflammation-related genes (*Tnfa* and *Il6*) in the indicated groups. For all statistical plots, the data are presented as mean ± S.E.M, and statistical significance is indicated as ns means not significant, $^{*}P < 0.05$, $^{**}P < 0.01$, $^{***}P < 0.001$. HFD, high-fat diet; TGs, triglycerides; ALT, alanine aminotransferase; AST, aspartate aminotransferase; GTTs, Glucose tolerance tests, ITTs: insulin tolerance tests; 3-MA: 3-methyladenine; HGF, hepatocyte growth factor

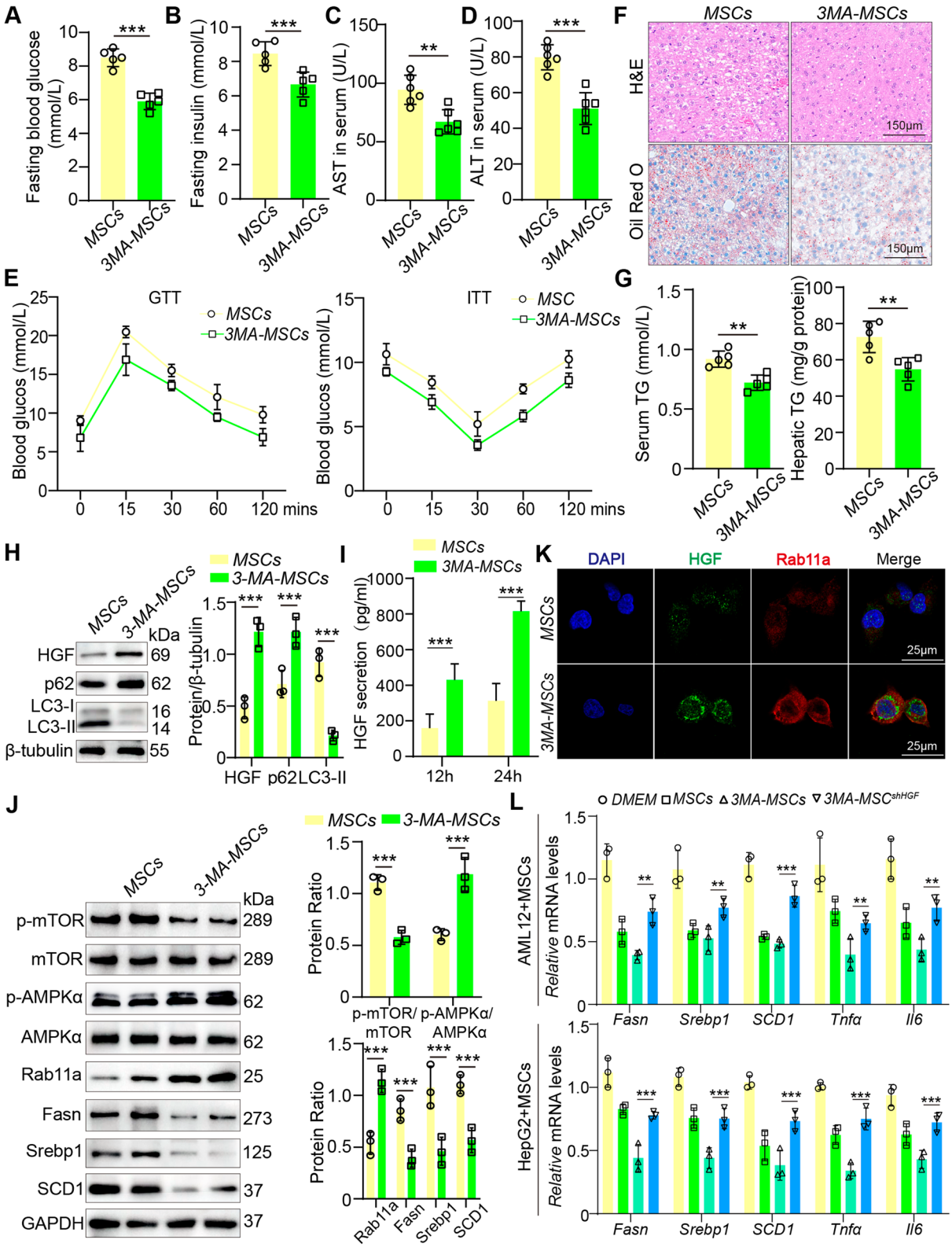

Fig. 7 (See legend on previous page.)

we found that MSCs with autophagy defects exhibit higher proliferative activity and characteristics that confer resistance to aging and apoptosis. Previous studies in other cell types have demonstrated that the loss of Atg5 inhibits autophagy and rescues cells from G0/G1 cell cycle arrest, thereby promoting cell proliferation [8, 32]. This ability to enhance the biological characteristics of MSCs, making them appear younger and more vigorous by inhibiting autophagy, may have significant implications for disease treatment.

Previous studies have demonstrated that MSCs from various sources can improve metabolic disorders associated with NAFLD [4, 33]. However, a critical scientific question remains: how can we genetically engineer MSCs to enhance their therapeutic effects in treating this disease? Enhancing therapeutic efficacy is often achieved by increasing the secretion of specific paracrine factors or by boosting the biological activity of the cells. In our research, we investigated the role of autophagy-deficient MSCs in a NAFLD model using both an in vitro co-culture system and a high-fat diet mouse model. Our results showed that autophagy-deficient MSCs significantly suppressed lipid synthesis in NAFLD. Furthermore, we discovered that these MSCs corrected the dysregulated AMPKα/mTOR/S6K/Srebp1 signaling pathway associated with the disease. However, we still lack a clear understanding of the direct targets of MSCs once they enter the mouse body, and the targets influenced by MSCs may be diverse and varied. Despite some studies identifying potential targets of MSCs in the host organism, it remains challenging to clarify their direct and indirect effects.

MSCs typically survive in the host for 7 days to 1 month, during which they can secrete a wide array of growth factors, chemokines, and inflammatory mediators [8, 27]. These factors serve as effector molecules that influence host cells. In our research, we conducted protein chip and ELISA assays on the supernatant secreted by MSCs and identified several factors with high expression levels, including Angiogenin, VEGF, HGF, and bFGF. Notably, we found that HGF was one of the factors that showed a significant increase in secretion from autophagy-deficient MSCs. This finding suggests that the Atg5-dependent autophagy defect selectively impacts the expression of protein factors secreted by MSCs. Furthermore, autophagy defects induced by other related molecules may result in distinct secretion profiles compared to those associated with Atg5 deficiency. HGF, a pleiotropic growth factor, influences lipid metabolism by promoting the mobilization and oxidation of fatty acids. Additionally, it is implicated in enhancing insulin sensitivity and exhibits anti-inflammatory properties [34, 35]. Therefore, our research indicates that Atg5-deficient MSCs enhance lipid metabolism disorders in NAFLD by promoting the secretion of HGF.

The process of vesicular transport includes both endocytosis and autophagy, which transport cellular materials to lysosomes for degradation and play a role in extracellular signaling. Recent studies have begun to uncover how endocytic and autophagic compartments can work synergistically to optimize the status of specific proteins within the cell [17]. Our findings indicate that Atg5-deficient MSCs exhibit a reduced number of EEs, LEs and lysosomes, while showing an increase in Rab11a-positive REs. The REs can encapsulate proteins and cellular metabolic products, ultimately reaching the cell membrane, where they fuse to release intracellular cargo and trigger a series of signaling pathways. In this study, we hypothesize that RE sorting activity is pronounced in Atg5-deficient MSCs, facilitating the extracellular delivery of HGF through endosomal sorting. While current evidence partially supports our hypothesis, several important questions remain to be addressed, including how HGF is selectively secreted into the extracellular space via REs and what its targets are in mice. In addition to the direct secretion of HGF, future studies should also explore whether HGF is contained in extracellular vesicles derived from MSCs. Addressing these questions will be crucial for enhancing our understanding of the roles of autophagy-modified MSCs in the context of NAFLD. In summary, our research presents a strategy to enhance the secretion of the effector factor HGF from MSCs through genetic engineering, thereby improving outcomes in metabolic liver diseases. This study provides new experimental data and treatment strategies for MSC-based therapy.

Abbreviations

MSCs	Mesenchymal stem cells
NAFLD	Non-alcoholic fatty liver disease
NASH	Non-alcoholic steatohepatitis
HGF	Hepatocyte growth factor
HFD	High-fat diet
FFAs	Free fatty acids
EdU	5-Ethynyl-2′-deoxyuridine
βgal	β-galactosidase
TGs	Triglycerides
ALT	Alanine aminotransferase
AST	Aspartate aminotransferase
GTTs	Glucose tolerance tests
ITTs	Insulin tolerance tests
NCD	Normal chow diet
3-MA	3-methyladenine
CQ	Chloroquine
REs	Recycling endosomes
EEs	Early endosomes
LEs	Late endosomes

Supplementary Information

The online version contains supplementary material available at https://doi.org/10.1186/s12964-024-01950-x.

Supplementary Material 1.

Authors' contributions

Caifeng Zhang: Conceptualization, Data curation, Funding acquisition, Investigation, Methodology, Validation, Writing-original draft, Writing – review & editing. Juanjuan Ji: Data curation, Investigation, Methodology. Xuefang Du: Data curation, Investigation, Methodology. Lanfang Zhang: Formal analysis, Investigation, Methodology. Yaxuan Song: Methodology. Yuyu Wang: Methodology. Yanan Jiang: Data curation, Formal analysis, Methodology. Ke Li: Data curation, Formal analysis, Methodology. Tingmin Chang: Project administration, Supervision.

Funding

This work was supported by grants from the research project on medical science and technology in Henan Province (LHGJ20210531).

Data availability

No datasets were generated or analysed during the current study.

Declarations

Competing interests

The authors declare no competing interests.

Author details

[1]Department of Gastroenterology, The First Affiliated Hospital of Xinxiang Medical University, Xinxiang, Henan Province, China. [2]First College for Clinical Medicine, Xinxiang Medical University, Xinxiang, Henan 453003, China. [3]Department of Pathophysiology, School of Basic Medical Sciences, College of Medicine, Zhengzhou University, Zhengzhou, Henan 450000, China.

Received: 2 September 2024 Accepted: 17 November 2024
Published online: 03 December 2024

References

1. Younossi Z, Anstee QM, Marietti M, Hardy T, Henry L, Eslam M, et al. Global burden of NAFLD and NASH: trends, predictions, risk factors and prevention. Nat Rev Gastroenterol Hepatol. 2018;15(1):11–20.
2. Friedman SL, Neuschwander-Tetri BA, Rinella M, Sanyal AJ. Mechanisms of NAFLD development and therapeutic strategies. Nat Med. 2018;24(7):908–22.
3. Du J, Ji Y, Qiao L, Liu Y, Lin J. Cellular endo-lysosomal dysfunction in the pathogenesis of non-alcoholic fatty liver disease. Liver Int. 2020;40(2):271–80.
4. Korkida F, Stamatopoulou A, Roubelakis MG. Recent Advances in Mesenchymal Stem/Stromal Cell-Based Therapy for Alcohol-Associated Liver Disease and Non-alcoholic Fatty Liver Disease. Stem Cells Transl Med. 2024;13(2):107–15.
5. Yang F, Wu Y, Chen Y, Xi J, Chu Y, Jin J, et al. Human umbilical cord mesenchymal stem cell-derived exosomes ameliorate liver steatosis by promoting fatty acid oxidation and reducing fatty acid synthesis. JHEP Rep. 2023;5(7): 100746.
6. Du J, Jiang Y, Liu X, Ji X, Xu B, Zhang Y, et al. HGF Secreted by Menstrual Blood-Derived Endometrial Stem Cells Ameliorates Non-Alcoholic Fatty Liver Disease Through Downregulation of Hepatic Rnf186. Stem Cells. 2023;41(2):153–68.
7. Hu C, Wu Z, Li L. Mesenchymal stromal cells promote liver regeneration through regulation of immune cells. Int J Biol Sci. 2020;16(5):893–903.
8. Du J, Zhu X, Guo R, Xu Z, Cheng FF, Liu Q, et al. Autophagy induces G0/G1 arrest and apoptosis in menstrual blood-derived endometrial stem cells via GSK3-beta/beta-catenin pathway. Stem Cell Res Ther. 2018;9(1):330.
9. Lopez-Yus M, Garcia-Sobreviela MP, Del Moral-Bergos R, Arbones-Mainar JM. Gene Therapy Based on Mesenchymal Stem Cells Derived from Adipose Tissue for the Treatment of Obesity and Its Metabolic Complications. Int J Mol Sci. 2023;24(8):7468.
10. Byrnes K, Blessinger S, Bailey NT, Scaife R, Liu G, Khambu B. Therapeutic regulation of autophagy in hepatic metabolism. Acta Pharm Sin B. 2022;12(1):33–49.
11. Filali-Mouncef Y, Hunter C, Roccio F, Zagkou S, Dupont N, Primard C, et al. The menage a trois of autophagy, lipid droplets and liver disease. Autophagy. 2022;18(1):50–72.
12. Du J, Ji X, Xu B, Du Q, Li Y, Zhou B, et al. Ubiquitination of cytoplasmic HMGB1 by RNF186 regulates hepatic lipophagy in non-alcoholic fatty liver disease. Metabolism. 2024;152: 155769.
13. Puri C, Manni MM, Vicinanza M, Hilcenko C, Zhu Y, Runwal G, et al. A DNM2 Centronuclear Myopathy Mutation Reveals a Link between Recycling Endosome Scission and Autophagy. Dev Cell. 2020;53(2):154–168 e156.
14. Noguchi S, Honda S, Saitoh T, Matsumura H, Nishimura E, Akira S, et al. Beclin 1 regulates recycling endosome and is required for skin development in mice. Commun Biol. 2019;2:37.
15. Pei Y, Lv S, Shi Y, Jia J, Ma M, Han H, et al. RAB21 controls autophagy and cellular energy homeostasis by regulating retromer-mediated recycling of SLC2A1/GLUT1. Autophagy. 2023;19(4):1070–86.
16. Carosi JM, Hein LK, Sandow JJ, Dang LVP, Hattersley K, Denton D, et al. Autophagy captures the retromer-TBC1D5 complex to inhibit receptor recycling. Autophagy. 2024;20(4):863–82.
17. Fraser J, Simpson J, Fontana R, Kishi-Itakura C, Ktistakis NT, Gammoh N. Targeting of early endosomes by autophagy facilitates EGFR recycling and signalling. EMBO Rep. 2019;20(10): e47734.
18. Tang Q, Liu W, Yang X, Tian Y, Chen J, Hu Y, et al. ATG5-Mediated Autophagy May Inhibit Pyroptosis to Ameliorate Oleic Acid-Induced Hepatocyte Steatosis. DNA Cell Biol. 2022;41(12):1038–52.
19. Hu Y, Li J, Li X, Wang D, Xiang R, Liu W, et al. Hepatocyte-secreted FAM3D ameliorates hepatic steatosis by activating FPR1-hnRNP U-GR-SCAD pathway to enhance lipid oxidation. Metabolism. 2023;146: 155661.
20. Niu Q, Wang T, Wang Z, Wang F, Huang D, Sun H, et al. Adipose-derived mesenchymal stem cell-secreted extracellular vesicles alleviate non-alcoholic fatty liver disease via delivering miR-223-3p. Adipocyte. 2022;11(1):572–87.
21. Feng J, Qiu S, Zhou S, Tan Y, Bai Y, Cao H, et al. mTOR: A Potential New Target in Nonalcoholic Fatty Liver Disease. Int J Mol Sci. 2022;23(16):9196.
22. Caron A, Richard D, Laplante M. The Roles of mTOR Complexes in Lipid Metabolism. Annu Rev Nutr. 2015;35:321–48.
23. Gong L, Wang Z, Wang Z, Zhang Z. Sestrin2 as a Potential Target for Regulating Metabolic-Related Diseases. Front Endocrinol (Lausanne). 2021;12: 751020.
24. Sun HJ, Wu ZY, Nie XW, Wang XY, Bian JS. Implications of hydrogen sulfide in liver pathophysiology: Mechanistic insights and therapeutic potential. J Adv Res. 2021;27:127–35.
25. Xue Z, Liao Y, Li Y. Effects of microenvironment and biological behavior on the paracrine function of stem cells. Genes Dis. 2024;11(1):135–47.
26. Du F, Liu M, Wang J, Hu L, Zeng D, Zhou S, et al. Metformin coordinates with mesenchymal cells to promote VEGF-mediated angiogenesis in diabetic wound healing through Akt/mTOR activation. Metabolism. 2023;140: 155398.
27. Kuppa SS, Kim HK, Kang JY, Lee SC, Seon JK. Role of Mesenchymal Stem Cells and Their Paracrine Mediators in Macrophage Polarization: An Approach to Reduce Inflammation in Osteoarthritis. Int J Mol Sci. 2022;23(21):13016.
28. Raudenska M, Balvan J, Masarik M. Crosstalk between autophagy inhibitors and endosome-related secretory pathways: a challenge for autophagy-based treatment of solid cancers. Mol Cancer. 2021;20(1):140.
29. Tognarelli EI, Reyes A, Corrales N, Carreno LJ, Bueno SM, Kalergis AM, et al. Modulation of Endosome Function, Vesicle Trafficking and Autophagy by Human Herpesviruses. Cells. 2021;10(3):542.
30. Mahapatra KK, Panigrahi DP, Praharaj PP, Bhol CS, Patra S, Mishra SR, et al. Molecular interplay of autophagy and endocytosis in human health and diseases. Biol Rev Camb Philos Soc. 2019;94(4):1576–90.
31. Garza Trevino EN, Quiroz Reyes AG, Delgado Gonzalez P, Rojas Murillo JA, Islas JF, Alonso SS, et al. Applications of Modified Mesenchymal

Stem Cells as Targeted Systems against Tumor Cells. Int J Mol Sci. 2024;25(14):7791.
32. Qin Y, Sun W, Zhang H, Zhang P, Wang Z, Dong W, et al. LncRNA GAS8-AS1 inhibits cell proliferation through ATG5-mediated autophagy in papillary thyroid cancer. Endocrine. 2018;59(3):555–64.
33. Hu J, Li S, Zhong X, Wei Y, Sun Q, Zhong L. Human umbilical cord mesenchymal stem cells attenuate diet-induced obesity and NASH-related fibrosis in mice. Heliyon. 2024;10(3): e25460.
34. Shaker ME, Gomaa HAM, Abdelgawad MA, El-Mesery M, Shaaban AA, Hazem SH. Emerging roles of tyrosine kinases in hepatic inflammatory diseases and therapeutic opportunities. Int Immunopharmacol. 2023;120: 110373.
35. Wu D, van de Graaf SFJ. Maladaptive regeneration and metabolic dysfunction associated steatotic liver disease: Common mechanisms and potential therapeutic targets. Biochem Pharmacol. 2024;227: 116437.

Publisher's Note